RESEARCH COMMUNICATION

Differential Protein Expression in EC304 Gastric Cancer Cells Induced by Alphastatin

Xin-Xin Wang[1&], Rong-Ju Sun[2&], Meng Wu[3], Tao Li[1], Yong Zhang[1], Lin Chen[1*]

Abstract

Objective: To explore the differential protein expression profile in EC304 gastric cancer cells induced by alphastatin. Methods: Cultured EC304 cells in the exponential phase of growth were randomly divided into alphastatin and control groups. Total proteins were extracted and the two dimensional electrophoresis (2-DE) technique was applied to analyze differences in expression with ImageMaster 2D Platinum 5.0 software. Proteins were identified using the MASCOT database and selected differently expressed proteins were characterised by western blotting and immunofluorescence. Results: 1350±90 protein spots were detected by the ImageMaster software in the 2-DE gel images from the control and alphastatin groups. The match rate was about 72-80% for the spectrum profiles, with 29 significantly different protein spots being identified, 10 upregulated, 16 downregulated, two new and one lost. The MASCOT search scores were 64-666 and the peptide matching numbers were 3-27 with sequence coverage of 8-62%. Twenty-three proteins were checked by mass spectrometry, including decrease in Nm23 and profilin-2 isoform b associated with the regulation of actin multimerisation induced by extracellular signals. Conclusion: The proteome in EC304 cells is dramatically altered by alphastatin, which appears to play an important role in modulating cellular activity and anti-angiogenesis by regulating protein expression and signal transduction pathways through Nm23 and profilin-2 isoform b, providing new research directions for anti-angiogenic therapy of gastric cancer.

Keywords: Alphastatin - EC304 gastric cancer cells - proteome - 2-DE - mass spectrometry - anti-angiogenesis

Asian Pacific J Cancer Prev, **13**, 1667-1674

Introduction

Angiogenesis, a prerequisite for the adequate blood supply, growth and metastasis of a tumour, is the process of forming new blood vessels based on existing ones. The process of angiogenesis includes the activation of endothelial cells, the degradation of the extracellular basement membrane and matrix in the local vasculature, the migration of vascular endothelial cells, endothelial cell proliferation, the rearrangement new extracellular matrix and the formation of vessel walls. Among these processes, endothelial cell migration, proliferation and tubule formation are the three most important aspects, and have been observed through in vitro experiments in previous studies (Capdevila et al., 2008). Under normal circumstances, these processes are regulated in a relative state of equilibrium. When disease occurs, the balance is broken by some angiogenic factors, resulting in abnormal blood vessel formation. Angiogenesis inhibitors exert their effects by inhibiting the release of angiogenic factors and through antagonistic action. The main mechanisms are inhibition of the vascular endothelial growth factor (VEGF) pathway and inhibition of cyclooxygenase 2 (COX-2) (Colorectal Cancer Collaborative Group, 2000). Angiogenesis is a prerequisite for the occurrence and development stomach cancer. Further study on the mechanism of gastric cancer angiogenesis will be helpful for early diagnosis, the evaluation of clinical prognosis and the exploration of anti-angiogenic treatments for gastric carcinoma (Hurwitz et al., 2004).

Alphastatin is 24-amino acid fragment of the α-chain end of human fibrinogen, which was first reported by the British researchers Lewis et al. In 2004, Carolyn et al. found that alphastatin could inhibit angiogenesis in vitro and tumour angiogenesis in mice (Ferrara and Davis-Smyth, 1997). Experiments revealed that alphastatin could inhibit angiogenesis in isolated vascular endothelial cells in vitro and murine CT26 tumour angiogenesis without side effects. Alphastatin, as a new angiogenesis inhibitor, strongly inhibits angiogenesis, so the exploration of its mechanism is helpful for the correct application of this compound. The study of alphastatin in vascular endothelial cells undergoing angiogenesis and its possible mechanism of action would be helpful for not only understanding the biological activity of alphastatin, but would also provide an alternative in the clinical treatment of gastric cancer (Ferrara and Davis-Smyth, 1997). Our previous experiments explored the effects of alphastatin on the

*[1]Department of General Surgery, [2]Department of Emergency, [3]Department of Plastic Surgery, Chinese People's Liberation Army General Hospital, Beijing, China [&]Equal contributors *For correspondence: linchen2001@yeah.net*

biological characteristics of human vascular endothelial cells. A further study observed the direct effects of alphastatin in cell migration, proliferation and tubular structures during angiogenesis. The results confirmed that alphastatin could inhibit the migration of vascular endothelial cells and the formation of tubular structures, but had no obvious effects on cell proliferation.

With the rapid development of proteomics, studies on gastric cancer angiogenesis and anti-angiogenic mechanisms may be performed. In the present study, we investigated the differences in protein expression by EC304 cells induced by alphastatin using proteomics technology, and identified different proteins by nanolitre ultra-high performance liquid chromatogram-electrospray ionisation tandem mass spectrometry. The results of this study provide a scientific basis for the mechanism of alphastatin in inhibiting gastric carcinoma angiogenesis, suggesting that this compound may be used as a biological anti-angiogenic therapy (Shevchenko et al., 1996; Candiano et al., 2004).

Materials and Methods

Materials and reagents

Alphastatin (ADSGEGDFLAEGGGVRGPR-VVERH) was purchased from Promega, and human umbilical vein endothelial cells (EC304 cells) were purchased from ATCC (USA). A solid phase pH gradient isoelectric focusing instrument (IPGphor IEF System), ImageMaster 2D platinum image analysis software and a gel image scanner (ImageScanner) were purchased from Amersham Pharmacia. Nanolitre ultra-high performance liquid chromatography-electrospray ionisation tandem mass spectrometry (NanoUPLC-ESI-MS/MS HDMS) equipment was purchased from Waters (USA).

EC304 cell culture

EC304 cells were cultured according to the conventional method in DMEM with 10% foetal bovine serum (Gibco, USA), with the addition of 100,000 U/L penicillin and 100 mg/L streptomycin. EC304 cells at a density of 2×10^4 cells/mL were seeded in 150 cm^2 plastic culture flasks at 37 ºC in a 5% CO_2 incubator. When the cell density reached 80% saturation of the logarithmic growth phase, EC304 cells were divided into experimental groups.

Experimental groups and procedures

When the cell density reached 80% saturation of the logarithmic growth phase, serum-free medium was used for 24 h with synchronous processing, then cells were randomly divided into two groups, the alphastatin group and the control group. In the alphastatin group, alphastatin was added to the cell culture flasks after dissolving it in serum-free DMEM to a final concentration of 10-7 to 10-10 mol/L; cells were subsequently maintained at 37 ºC in a 5% CO_2 incubator. In the control group, the equivalent volume of normal saline was added to the cell culture flasks under the same experimental conditions.

2D and SDS-polyacrylamide gel electrophoresis (SDS-PAGE)

In both groups, cells were washed twice with PBS after 24 h of culture and digested with 0.25% trypsin, centrifuged and washed with PBS. The cells were then collected into Eppendorf tubes. The protein extraction agent, composed of 40 mmol/L Tris-base, 7 mol/L urea, 2 mol/L thiourea, 4% CHAPS, 1% DTI, 1 mmol/L EDTA, 25 g/ml protease inhibitor cocktail and 20 g/mL PMSF, was used at a ratio of 1:3.5. Cells were fully fragmented in an ice bath and freeze-thawing was performed in liquid nitrogen three times. Next, 20 μL of 10 μg/mL DNAse and 7 μL 2.5 μg/mL RNAse were added to the tube and gently mixed. The tubes were then placed in an ice bath for 20 min, then centrifuged for 20 min at 14,000 rpm at 4 ºC. The supernatants were stored at -70 ºC after protein quantification by the Bradford method (Coomassie brilliant blue). Proteins were extracted in amounts of 100-150 g (silver staining) or 1.0-1.5 mg (Coomassie staining) with 20 mM DTT, 0.5% IPG buffer and heavy swelling liquid to a final volume of 350 μL. Cells were then oscillated, centrifuged, and defoamed, then added to the IPG gel tank. The gel strip (18 cm, pH 3-10, NL) was immersed in the sample solution with the gel surface facing down, covered with 800 μL of mineral oil (drystrip cover fluid), then placed in the solid phase pH gradient isoelectric focusing instrument (panel temperature 20 ºC, 50 mA/strip, 30 V for 10 h, 2000 V for 30 min, 5000 V for 30 min, 8000 V for 10 h or 80000 V for Hs). The IPG gel strip was transferred to the top of a 13% polyacrylamide resin (20 cm × 20 cm × 1 mm) with the surface up, the acidic side on the left and the alkaline side on the right. Several markers (97000, 66000, 45000, 30000, 20100 and 14000) were used. The gel strip was sealed with 0.5% agarose and cooled to 19 ºC. The operating parameters of the PROTEANCxi cell were 20 mA/gel for 40 min and 30 mA/gel until the bromophenol blue reached the edge of the glass plate. After bleaching, the strip was scanned by a gel image scanner, which was analysed by ImageMaster 2D Platinum software. Protein expression was calculated by grouping statistical tools.

Protein identification by nanoUPLC-ESI-MS/MS

The following HPLC conditions were used in the present study: the instrument used was a nanoACQUITY UPLC (Waters), the enrichment column was Symmetry C18, with dimensions of 180 μm x 20 mm and 5 μm particles, the analytical column for ultra high-performance liquid chromatography mix-particles column linkage with methylmethane (BEH C18, 75 μm × 250 mm, 1.7 μm particles), the column temperature was 35 ºC and the flow rate was 200 nL/min. Mobile phase A included 0.1% formic acid and mobile phase B included acetonitrile containing 0.1% formic acid. The gradients were 1% to 40% B for 80 min, 40% to 80% B for 10 min, hold with 80% B for 10 min, balance for 20 min, then the initial of 1% B. The ionisation mode of positive ion nano-electrospray and DDA data acquisition mode were used, and the two highest intensity ions were analysed by tandem mass spectrometry in each scan. The capillary voltage was 2500 V, the cone voltage was 35 V and the source temperature was 90 ºC in the range of MS 350-1600 and MS/MS 50-2000. The data analysis software used was

PLGS v2.3, and the database for the MASCOT index was used in MS/MS ion mode. Our study set the index terms as trypsin digestion, M oxide and indoacetamide alkylation of variable modifications and a missed cut site of 1. The quality error of MS and MS/MS was 0.2 Da. The NCBInr database was used.

Western blotting

EC304 cells were routinely cultured and passaged. After three passages, cells were transferred into 6-well plates, and randomly divided into two groups until 80% confluence (n=3). Next, 70 μg/mL or 100 μg/mL alphastatin was added to the medium (DMEM) in the alphastatin group, and simple DMEM medium was added in the control group. These groups were cultured for another 24 h, and the medium was removed after 48 h. After two washes with cold PBS buffer, 200 μL of RIPA protein buffer were added for full cell lysis in an ice bath. Disrupted cells were transferred to a pre-cooled Eppendorf tube, then centrifuged at 12000 g and 4ºC for 15 min. The supernatant was transferred to another pre-cooled Eppendorf tube, and the protein concentration was determined by the Coomassie brilliant blue method. The samples were then stored at -80 ºC. A 5% SDS-PAGE gel and a 5% spacer gel were prepared, and 30 μg of the protein sample were added in each well for 80 V and 120V electrophoresis. Electrophoresis continued for 30 min after the indicator front entered the buffer (a total running time of about 2.5 h). After electrophoresis, the proteins from the SDS-PAGE gel were transferred to a nitrocellulose membrane at 120 V in an ice bath for 180 min, stained with Ponceau reagent for the observation of protein bands, then washed with TBST. After blocking with 5% skim milk at room temperature for 1 h, the membranes were incubated with primary antibodies at 4 ºC overnight (Abcam, 1:1000), washed with TBST three times (10 min for each wash), then hybridised with the secondary HRP-tagged antibody at room temperature for 1 h (Zhongshan Goldenbridge, 1:3000), followed by three TBST washes. The membrane was tiled on the refreshing film, ECL ultra-sensitive light-emitting solution was added, and the film was exposed in the darkroom. Finally, the greyscale intensity of the bands was analysed.

Immunofluorescence

EC304 cells were routinely cultured and passaged. After three passages, cells were digested with trypsin, and a single cell suspension was prepared and cells were randomly divided into two groups. The cell suspension was dropped on a slide in a 6-well plate, and cultured at 37 ºC in a 5% carbon dioxide incubator for 24 h. The slides were washed three times with PBS at 37 ºC (each wash was 3 min), then fixed in 4% paraformaldehyde for 15 min and washed with deionised water at 37 ºC. The climbing film was dried on filter paper, glued on the glass slide with gum, then fixed in 4% paraformaldehyde for 10 min, followed by a 5 min PBS wash and permeabilisation with 0.5% Triton for 15 min, followed by two more PBS washes. The cells were sealed with confining liquid at room temperature for 30 min, incubated with the primary antibody at 4 ºC overnight, equilibrated to room temperature for 10 min, washed with PBST three times (5 min each). Cells were incubated with the fluorescently labelled secondary antibody at room temperature in the dark for 1 h, then rinsed with PBST three times (5 min each). After washing with distilled water, the slide was coverslipped with mounting media, and images were obtained by fluorescence microscopy.

Results

EC304 cell proliferation and tubular structures

In agreement with our previous study, we confirmed that alphastatin prevents angiogenesis in vitro by inhibiting endothelial cell migration and the formation of tubular structures (Figure 1).

2D electropherogram and image analysis

Stable, repetitive, high resolution and low interference two-dimensional gel electrophoresis was established in this study. At least five electrophoresis experiments were repeated for each sample, and images were analysed by ImageMaster 2D platinum version 5.0 after silver staining. About 1350 ± 90 protein spots were detected in each gel (Figure 2), and the match rate of gels reached 70-82%.

Differential analysis of two-dimensional gel electrophoresis

The differential analysis was carried out between the control group and the alphastatin group in EC304 cells, and the relative amounts of each protein and the relative strength ratio value (protein spot value/central tendency) of each protein spot in different gels were calculated.

Figure 3A shows the differential point matching images from the ImageMaster software, showing an overlapping image of the control group and the alphastatin group. In these images, red circles represent protein spots automatically identified by the software in the control group, while the blue circles represent protein spots automatically identified by the software in the alphastatin

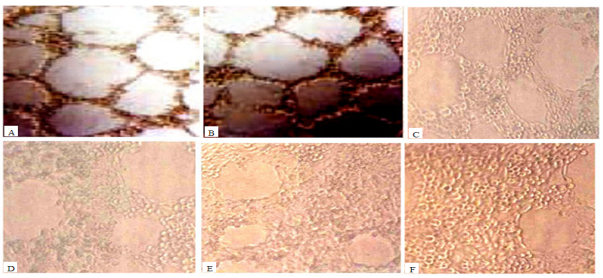

Figure 1. 2-DE image of Different Proteins Expressed in EC304 Cells. A: Control, B: 0 nM alphastatin, C: 25 nM alphastatin, D: 50 nM alphastatin, E: 75 nM alphastatin, F: 100 nM alphastatin

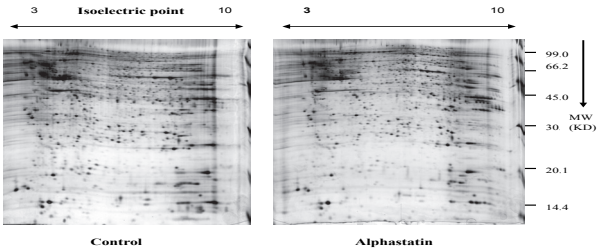

Figure 2. 2-DE Image of Different Proteins Expressed in EC304 Cells. Control, the control group; alphastatin, the alphastatin group

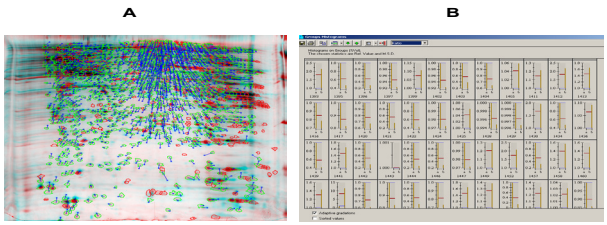

Figure 3. Image Analysis of Different Spots. A: the matching image of different spots, B: the distribution of the relative amount of the different spots

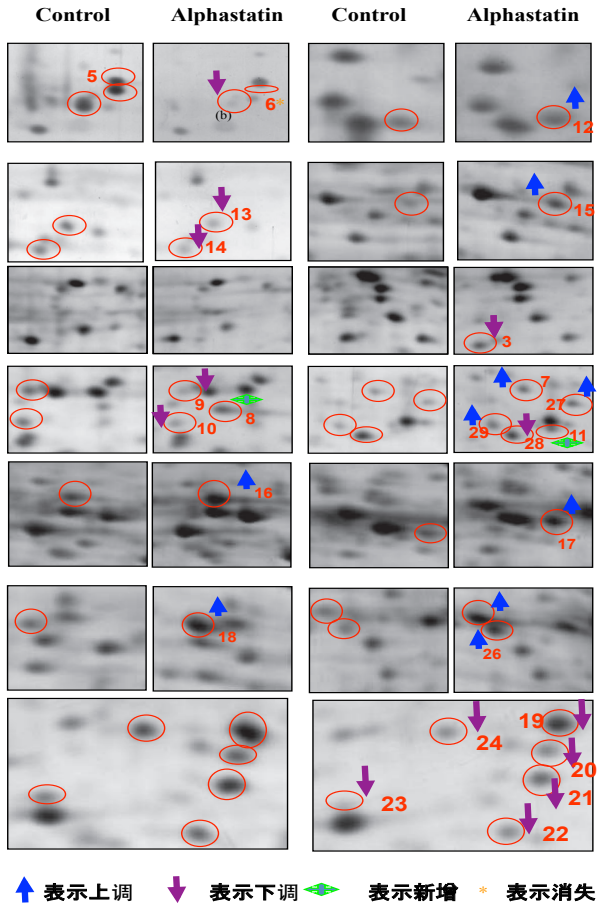

Figure 4. Different Protein Spots. Control, the control group; alphastatin, the alphastatin group

group. One pair is shown as a blue vector connecting the protein locations of the stacking gel.

Figure 3B shows the distribution ratio of the relative amounts of some corresponding spots of different proteins. The total number of differential spots was 29, with a changing multiple > 3; these included 12 upregulated spots, with a maximum multiple of 25, and 17 downregulated spots, with a maximum multiple of 0.1.

Differentiation of protein spots

Through the analysis by the ImageMaster software and subsequent verification, 29 protein spots with significant differences were found in the alphastatin group ($p < 0.05$), including 10 upregulated protein spots, 16 downregulated protein spots, two new protein spots (8 and 11) and one lost protein spot (6). The upregulation multiple was about 3- to 25-fold, and the lowest downregulation multiple was about 0.1-fold (Figure 4).

Identification of different protein spots

Table 1. The Nine Peptides, and Related Information Match on Differentially Expressed Proteins

Start - end	Molecular weight	Errors(Da)	Amino acid of peptides
34 - 49	639.9863	0.0044	K.SIQEIQELDKDDESLR.K
51 - 58	475.2719	-0.01	K.YKEALLGR.V
99 - 105	425.2567	-0.0131	K.KQSFVLK.E
112 - 117	382.2407	-0.0083	R.IKISFR.V
121 - 127	382.2042	-0.0007	R.EIVSGMK.Y
128 - 134	490.7501	-0.0019	K.YIQHTYR.K
139 - 152	801.387	0.0039	K.IDKTDYMVGSYGPR.A
142 - 152	623.2852	0.0063	K.TDYMVGSYGPR.A
153 - 167	876.4221	-0.0005	R.AEEYEFLTPVEEAPK.G

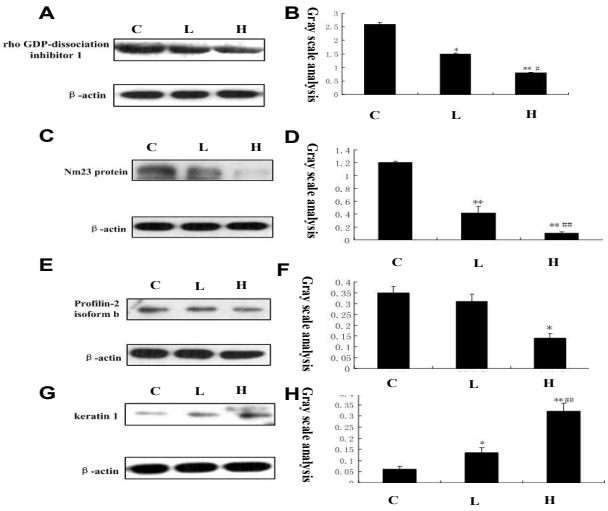

Figure 5. The Expressions of Rho GDP-dissociation Inhibitor 1, Nm23, Profilin-2 Isoform b, and Translation Initiation Factor after the Treatment of Alphastatin. C, control group; L, low dose alphastatin group; H, high dose alphastatin group

NanoUPLC-ESI-MS/MS analysis: After silver staining, different protein spots were analysed by nanoUPLC- ESI-MS/MS, and the MASCOT index was obtained with the results of partial peptide sequencing. Twenty-nine different protein spots were selected with good reproducibility in mass spectrometry-compatible silver-stained gels, including 12 upregulated proteins and 17 downregulated proteins. The 29 proteins were identified by silver staining-nanoUPLC-ESI-MS/MS. The scores of MASCOT index were from 64 to 666 and the number of matching peptides was from 3 to 27. The rate of sequence coverage was 8% to 62%. Figure 4 shows nine peptides matching with differential protein spot 1; their sequence information is shown in Table 1, indicating 39% sequence coverage rate and a MASCOT database score of 469 points, which indicates that the result was reliable. The protein spot was identified as Rho GDP-dissociation inhibitor 1 isoform-a, which is a protease that dissociates GDP from Rho (Figure 5). Twenty-nine protein spots were identified as 23 different proteins (Table 2).

Effects of alphastatin on the expression of target proteins

After the administration of alphastatin for 24 h, the expression of Rho GDP-dissociation inhibitor 1 isoform a and Nm23 was significantly reduced, with a more significant decrease seen in the high dose alphastatin

Table 2.

Spot No.	Acc No.	Protein Name	Mr	pI	Score	Sequence Coverage(%)	Queries matched	Expression
1	gil4757768	rho GDP-dissociation inhibitor 1 isoform a calpain small subunit 1	23193	5.02	160	39	9	lower
2	gil4502565	Calcium-dependent protease	28298	5.05	64	12	3	
3	gil4929769	CGI-150 protein glyoxalase	54977	8.99	266	19	14	lower
6	gil35068	Nm23 protein nucleoside phosphorylating kinaseA	20398	7.07	297	45	13	lower
9	gil4929649	CGI-90 protein glyoxalase	35693	8.57	95	15	6	lower
10	gil180637	L-isoaspartyl/D-aspartyl protein carboxyl methyltransferase	24664	6.05	204	20	4	lower
11	gil16924265	Enoyl Coenzyme A hydratase 1, peroxisomal Enoyl-coA hydrolase	35735	8.47	264	19	7	Higher
		Chain A, Human Purine Nucleoside Phosphorylase Double Mutant E201q, N243d Complexed With 2-Fluoroadenine						
12	gil6912582	peflin calcium-binding protein	30361	6.1	177	15	8	Higher
	gil16751921	dermcidin preproprotein Dermcidin precursor	11277	6.08	136	22	3	
13	gil4505751	profilin-2 isoform b signal regulatory protein	15078	5.78	180	25	5	Lower
14	gil14249348	thioredoxin domain-containing protein 17 dithio-reducing enzyme	12932	5.4	166	26	3	Lower
16	gil5690372	glutaminase C	65430	8.09	246	8	4	Higher
17	gil496902	translation initiation factor	46803	6.08	104	19	11	Higher
19	gil2204207	glutathione S-transferase	23367	5.43	666	62	18	Lower
24	gil13398328	inosine triphosphate pyrophosphatase inosing triphosphatase hydratase	21485	5.78	268	34	7	Lower
25	gil460771	hnRNP-E1 RNA combinated protein	37502	6.66	395	39	16	Higher
26	gil460771	hnRNP-E1	37502	6.66	166	20	6	Higher
	gil4757880	mitotic checkpoint protein BUB3 isoform a	37131	6.36	150	18	6	
27	gil625039	elongation factor Ts	31871	7.14	101	16	5	Higher
28	gil4506179	proteasome subunit alpha type-1 isoform 2	29822	615	433	52	27	Lower
29	gil387033	purine nucleoside phosphorylase	32154	7.09	127	16	5	Higher

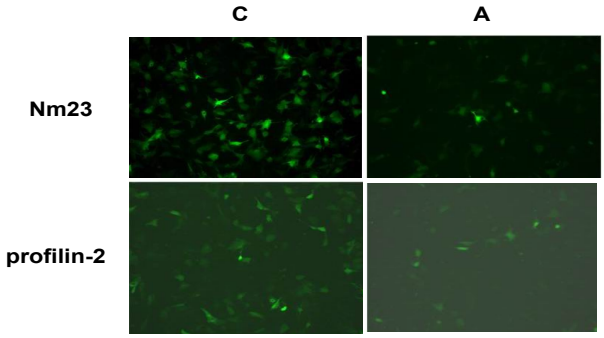

Figure 6. The Expression of Nm23 Protein and profilin-2 Isoform b after the Treatment of Alphastatin.
C, control group; A, alphastatin

group. Profilin-2 isoform b expression also showed a significant decrease, evident in the cytoplasm. Translation initiation factor expression showed a significant increase, again more significant in the high dose alphastatin group. Fluorescent expression of Nm23 protein was also significantly decreased in the cytoplasm of EC304 cells.

Discussion

Alphastatin, a 24-amino acid fragment of the human fibrinogen α-chain, was first reported by British scholars Lewis et al., who named it "alphastatin" (Hicklin and Ellis, 2005). In 2004, Carolyn et al. found that alphastatin could inhibit angiogenesis in vitro, and could inhibit tumour angiogenesis in mice (Groves et al., 2010). Experiments revealed that alphastatin could inhibit angiogenesis by vascular endothelial cells in vitro as well as murine CT26 tumour angiogenesis without side effects, showing good potential (Raffaniello et al., 2009). Alphastatin, as a new angiogenesis inhibitor, strong inhibits angiogenesis, and the exploration of its mechanism is helpful for the correct application of this compound. The study of alphastatin in vascular endothelial cell angiogenesis and its mechanisms of action would be helpful for not only understanding alphastatin biological activity, but might also provide an alternative in the clinical treatment of gastric cancer (Nakamura et al., 2006). Our previous experiments explored the effects of alphastatin on the biological characteristics of human vascular endothelial cells. Further study showed the direct effects of alphastatin in cell migration, proliferation and the formation of tubular structures during angiogenesis. These results showed that alphastatin can inhibit the migration of vascular endothelial cells and the formation of tubular structures, but has no obvious effects on cell proliferation (Ohira et al., 2005).

Previous experiments regarding vascular endothelial cell growth by two-dimensional electrophoresis need to be improved in terms of atlas reproducibility and sensitivity (Raffaniello and Raufman, 1999). In the present study, we established stable, repetitive, high resolution and low interference two-dimensional gel electrophoresis technology to evaluate EC304 cells. In order to obtain reliable electrophoretic patterns, EC304 cells were divided into the normal control group and the alphastatin group, with five biological replicates. The average protein spot in our study was more 300 points than the result of the literature (Marino and Zollo, 2007). Through the verification of proteins, there were 29 protein spots related to endothelial cell growth and endothelial cells, with 3- to

25-fold changes in expression, including 10 upregulated protein spots, 16 downregulated protein spots, two new protein spots and one lost protein spot. Generally speaking, the number of different proteins affected by alphastatin in EC304 cells was less than what was expected. The possible reasons were analysed as follows. In the present study, we choose a three-fold change as the standard for selecting different protein spots, but some spots with a less than three three-fold change may have a significant biological role which needs to be confirmed by further experiments. Additionally, a few proteins with significant quantitative changes may play an important role of inhibiting angiogenesis in gastric cancer (Tee et al., 2006).

The biological functions of different proteins from this identification include cell survival, senescence, apoptosis, stress response, energy metabolism, signal transduction and the ubiquitin pathway. Studies in the literature demonstrate that Rho GDP-dissociation inhibitor 1 isoform a regulates the GDP/GTP exchange reaction by inhibiting GDP dissociation from Rho (Almo et al., 1994; Taharaet al., 1998; Devineni et al., 1999; Di Nardo et al., 2000). This protein participates in a variety of biological activities, such as Rho-mediated signal transduction, apoptosis inhibition, axon production and cell adhesion, and is related to the nerve growth factor receptor signalling pathway. The nuclear chloride channel could make the cell membrane more stable and regulate intracellular pH and cell volume by epithelial cell transporting. The calcium-dependent protease of calpain small subunit 1 can be activated by calcium and oxidative stress. The calcium-binding protein peflin and programmed cell death gene 6 form a heterodimer, which regulates the function of calcium signalling. Profilin-2 isoform b regulates actin polymerisation induced by extracellular signals, which could affect the cytoskeletal structure.

Heterogeneous ribonucleoprotein E1 (hnRNP-E1) is an RNA-binding protein in the nucleus, and can be combined with mRNA, with effects on mRNA metabolism and transport. Inosine triphosphate pyrophosphatase can hydrolyse inosine triphosphate, regulating the intracellular ITP concentration.

Dual phosphorylation of nucleoside kinase A (Nm23) has a role in nucleoside triphosphate addition, and is involved in cell proliferation, differentiation and development, signal transduction, G protein-coupled receptor-mediated endocytosis and gene expression, all of which are very important in neural development, including neural patterns and cell fate (Akagi et al., 2003; Hao-AiShui et al., 2007; Lincoln et al., 2007; Cervantes et al., 2008; Fan et al., 2009).

Purine nucleoside phosphorylase catalyses the phosphorylation of purine nucleosides. Aspartic acid protein carboxyl methyltransferase (L-isoaspartyl/D-aspartyl protein carboxyl methyltransferase) can repair damaged proteins containing L-isoaspartyl and D-aspartatyl. Enoyl-coA hydrolase (enoyl coenzyme A hydratase 1, peroxisomal) has a peroxisomal targeting sequence in its C-terminus, and is therefore located in the peroxisome, and has effects on the auxiliary steps of fatty acid beta-oxidation. Disulphide reductase (thioredoxin domain-containing protein 17) contains the thioredoxin domain of protein 17, and regulates the signal activation of TNF-α and NF-ϰB, which contributes to cellular superoxide elimination. Glutaminase C catalyses the conversion of glutamic acid into glutamine with a possible role in neurotransmitter release (Inai et al., 2004; Willett et al., 2004).

The function of protein 4 with a glyoxal enzyme domain (CGI-150 protein GLOD4 and CGI-90 protein GLOD4) is still not clear. Purine nucleoside phosphorylase (chain A, human purine nucleoside phosphorylase double mutant E201q, N243d complexed with 2-fluoroadenine) catalyses the phosphorylation of purine nucleosides; a mutation in this protein may lead to immune dysfunction and nerve tissue disorders. Dermcidin preproprotein, the precursor of dermcidin, is a secreted protein with anti-bacterial and anti-fungal activity at the C-terminal, and its N-terminal can promote the survival of nerve cells under extreme oxidative stress. Glutathione S-transferase is formed by a variety of endochylema, mitochondria and microsomal proteins, and catalyses the combination of the reduced state of glutathione and the electrophilic centre of various substrates with an important role in cell detoxification.

Translation initiation factor is involved in the early steps of protein synthesis (Patel et al., 2003; Tong et al., 2004). The elongation factor of mitochondrial gene translation catalyses the exchange of guanine on the transcription elongation factor Tu in mitochondrial protein translation; its mutation causes a deficiency in oxidative phosphorylation. The protein BUB3 has a function at the mitotic checkpoint, with an important role in mitochondrial function. There are considerable proteasome subunit alpha type-1 isoforms in this cell type, which can cut proteins.

Recent studies have shown that Nm23 is expressed in different tumour cells, and that differential expression may be associated with tumour invasion and metastasis. There is high expression of Nm23 in gastric cancer cells, and the rate of positive expression is inconsistent in different histological types. The expression of Nm23 is higher in gastric cancer than other histological types of tubular adenocarcinoma, which may relate to its regulation of tumour cell formation. The positive expression rate of Nm23 is determined to some extent by the differentiation degree, as poorly differentiated cells show decreased expression, and there are significant differences in well-differentiated and moderately-differentiated cells compared to poorly differentiated cells. Some researchers think Nm23 is a differentiation gene, which contributes to the differentiation of tumour cells and a reduction in the degree of malignancy (Wildiers et al., 2003). Nrn23 expression is significantly correlated with the invasion depth of gastric cancer; it may be that Nm23 expression requires a certain stimulus and priming process. There is no Nm23 expression at the early stages of tumour formation, but with the progression of the tumour, certain stimuli or mechanisms promote Nm23 expression, with more expression in infiltrating and developed tumours. On the other hand, Nm23 stimulates the anti-inhibition mechanism in the tumour, which decreases or even abrogates the expression of this protein. Nm23 expression

is correlated with metastasis to the lymph nodes. Nm23 expression is significantly higher in lymph node negative cancer compared to cancer with lymph node metastases, which indicates that Nm23 is involved in the regulation of lymph node metastasis in gastric cancer. One possible reason for this is that Nm23 participates in cell microtubule maintenance and depolymerisation and in the regulation of some genes, especially Ras, ELa, etc.; thus, it plays negative regulatory role in tumour metastasis (Jain, 2005).

The present study confirmed that Nm23 expression was decreased by alphastatin in EC304 cells, and the expression of this protein was significantly reduced with an increase in the concentration of alphastatin. Alphastatin treatment led to the loss or mutation of Nm23, which is considered to be a tumour metastasis suppressor gene and could play a role in tumour angiogenesis. Nm23 may repress tumour metastasis by inhibiting angiogenesis (Gordon et al., 2001). Alphastatin may therefore play a role in inhibiting tumour vessel development by its effect on Nm23, eventually restraining tumour angiogenesis. These results provide a new direction for further study on Nm23 and Ras.

Our previous study found that many signalling pathways play a role in tumour angiogenesis. The DLL4/Notch signalling pathway regulates tumour angiogenesis. It has been found that high VEGF expression in tumour tissue promotes DLL4 expression in the membrane of vascular endothelial cells. DLL4 bound to the Notch receptor downregulates the endothelial cell response to VEGF by communicating with flanking cells, which leads to the inhibition of angiogenesis and a reduction in vascular branch formation. Inhibitors of DLL4 block the DLL4/Notch signalling pathway, which relieves the DLL4-mediated inhibition of vascular endothelial cell angiogenesis and vascular branch formation, resulting in an increase in blood vessel density in tumour tissue. The DLL4/Notch signalling pathway is regulated by VEGF, and together these two pathways regulate vascular endothelial sprouting, the formation of tubular structures and the maturation of new blood vessels into an effective vascular network.

Several characteristics differentiate tumour tissue angiogenesis from physiological angiogenesis. (1) Uncontrolled angiogenesis. Tumour angiogenesis is rapid and persistent. Approximately 10% to 20% of tumour vascular endothelial cells are in a state of DNA synthesis and mitochysis, as persistent angiogenesis is caused by the continuing high expression of tumour angiogenic factors. (2) Immature and easy penetration of blood vessels in tumour tissue. Histopathology shows that the lumen of new tumour vessels is irregular, with sinus-like expansions, thin vessel walls, a meagre or absent basement membrane, rare associated pericytes or smooth muscle cells, poor development into venules and arterioles, and the vessels have no contractile function without neurohumoral regulation. (3) Rich intratumoural microvessels. Research has found that the rate of tumour cell renewal is double that of vascular endothelial cells, and tumour microvessels are relatively inefficient and inadequate for this rate of tumour growth, such that the centre of the tumour often appears necrotic due to ischaemia and hypoxia. Blockade of the DLL4/Notch signalling pathway further strengthens the abovementioned characteristics of tumour angiogenesis.

The present study found that alphastatin could downregulate the expression of Rho GDP-dissociation inhibitor 1 isoform a in EC304 cells, which regulates the GDP/GTP exchange reaction by inhibiting GDP dissociation from Rho. Rho GDP-dissociation inhibitor 1 isoform a (GDI1) is an important protein in the Rho signalling pathway, and plays a significant role in inhibiting apoptosis, regulating axonal growth and cell adhesion, and participates in the nerve growth factor receptor signalling pathway.

The GDI1/Rho signalling pathway may reduce the number of new vessels by inhibiting excessive proliferation, and improve vascular function by promoting the development and maturation of new vessels. The relationship and role of the GDI1/Rho signal transduction pathway and VEGF in angiogenesis will be emphasised in further research. Additional study on the signalling pathways of angiogenesis will be helpful for providing new methods of inhibiting tumour angiogenesis and provide new directions for anti-tumour therapy.

References

Akagi M, Kawaguchi M, Liu W, et al (2003). Induction of neuropilin-1 and vascular endothelial growth factor by epidermal growth factor in human gastric cancer cells. *Br J Cancer,* **88**, 796-802.

Almo SC, Pollard TD, Way M, et al (1994). Purification, characterization and crystallization of Acanthamoeba profiling expressed in Escherichia coli. *J Mol Biol*, **236**, 950-2.

Bergers G, Benjamin LE (2003). Tumorigenesis and the angiogenic switch. *Nat Rev Cancer*, **3**, 401-10.

Candiano G, Bruschi M, Musante L, et al (2004). Blue silver: a very sensitive colloidal Coomassie G-250 staining for proteome analysis. *Electrophoresis*, **25**, 1327-33.

Capdevila J, Elez E, Peralta S, et al (2008). Oxaliplatin-based chemotherapy in the management of colorectal cancer. *Expert Rev Anticancer Ther*, **8**, 1223-36.

Cervantes A, Rosello´ S, Roda D, et al (2008). The treatment of advanced gastric cancer: current strategies and future perspectives. *Ann Oncol*, **19**, v103-7.

Colorectal Cancer Collaborative Group (2000). Palliative chemotherapy for advanced colorectal cancer: systematic review and meta-analysis. *BMJ*, **321**, 531-5.

Devineni N, Minamide LS, Niu M, et al (1999). Quantitative analysis of G-actin binding proteins and the G-actin pool in developing chick brain. *Brain Res*, **823**, 129-40.

Di Nardo A, Gareus R, Kwiatkowski D, et al (2000). Alternative splicing of the mouse profilin II gene generates functionally different profilin isoforms. *J Cell Sci*, **113**, 3795-803.

Fan S, Ramalingam SS, Kauh J, et al (2009). Phosphorylated eukaryotic translation initiation factor 4 (eIF4E) is elevated in human cancer tissues. *Cancer Biol Ther*, **8**, 1463-9.

Ferrara N, Davis-Smyth T (1997). The biology of vascular endothelial growth factor. *Endocr Rev*, **18**, 4-25.

Gordon MS, Margolin K, Talpaz M, et al (2001). Phase I safety and pharmacokinetic study of recombinant human anti-vascular endothelial growth factor in patients with advanced cancer. *J Clin Oncol*, **19**, 843-50.

Groves E, Rittinger K, Amstutz M, et al (2010). Sequestering of Rac by the Yersinia effector YopO blocks Fcgamma receptor-mediated phagocytosis. *J Biol Chem*, **285**, 4087-98.

Hao-AiShui, Shung-TaiHo, Jhi-Joung Wang, et al (2007). Proteomic analysis of spinal protein expression in rats exposed to repeated intrathecal morphine injection. *Proteomics*, **7**, 796-803.

Hicklin DJ, Ellis LM (2005). Role of the vascular endothelial growth factor pathway in tumor growth and angiogenesis. *Clin Oncol*, **23**, 1011-27.

Hurwitz H, Fehrenbacher L, Novotny W, et al (2004). Bevacizumab plus irinotecan, fluorouracil and leucovorin for metastatic colorectal cancer. *N Engl J Med*, **350**, 2335-42.

Inai T, Mancuso M, Hashizume H, et al (2004). Inhibition of vascular endothelial growth factor (VEGF) signaling in cancer causes loss of endothelial fenestrations, regression of tumor vessels, and appearance of basement membrane ghosts. *Am J Pathol*, **165**, 35-52.

Jain RK (2005). Normalization of tumor vasculature: an emerging concept in antiangiogenic therapy. *Science*, **307**, 58-62.

Lincoln DT, Singal PK, Al-Banaw A (2007). Growth hormone in vascular pathology: neovascularization and expression of receptors is associated with cellular proliferation. *Anticancer Res*, **27**, 4201-18.

Marino N, Zollo M (2007). Understanding h-prune biology in the fight against cancer. Clin Exp Metastasis, **24**, 637-45.

Nakamura K, Zhang X, Kuramitsu Y, et al (2006). Analysis on heat stress-induced hyperphosphorylation of stathmin at serine 37 in Jurkat cells by means of two-dimensional gel electrophoresis and tandem mass spectrometry. *J Chromatogr A*, **1106**, 181-9.

Nakamura T, Tabuchi Y, Ohno M (1998). Relations of nm23 expression to clinicopathologic variables and proliferative activity of gastric cancer lesions. *Cancer Detect Prev*, **22**, 246-50.

Ohira K, Kumanogoh H, Sahara Y, et al (2005). A truncated tropomyosin-related kinase B receptor, T1, regulates glial cell morphology via Rho GDP dissociation inhibitor 1. *J Neurosci*, **25**, 1343-53.

Patel N, Sun L, Moshinsky D, et al (2003). A selective and oral small molecule inhibitor of vascular epithelial growth factor receptor (VEGFR)-2 and VEGFR-1 inhibits neovascularization and vascular permeability. *J Pharmacol Exp Ther*, **306**, 838-45.

Raffaniello R, Fedorova D, Ip D, et al (2009). Hsp90 Co-localizes with Rab-GDI-1 and regulates agonist-induced amylase release in AR42J cells. *Cell Physiol Biochem*, **24**, 369-78.

Raffaniello RD, Raufman JP(1999). Cytosolic RAB3D is associated with RAB escortprotein (REP), not RAB-GDP dissociation inhibitor (GDI), in dispersed chief cells from guinea pig stomach. *J Cell Biochem*,**72**, 540-8.

Shevchenko A, Wilm M, Vorm O, et al (1996). Mass spectrometric sequencing of proteins from silver stained polyacrylamide gels. *Anal Chem*, **68**, 850-85.

Tahara E (2004). Genetic pathways of two types of gastric cancer. *IARC Sci Publ*, **157**, 327-49.

Tee YT, Chen GD, Lin LY, et al (2006). Nm23-H1: a metastasis-associated gene. *Taiwan J Obstet Gynecol*, **45**, 107-13.

Tong RT, Boucher Y, Kozin SV, et al (2004). Vascular normalization by vascular endothelial growth factor receptor 2 blockade induces a pressure gradient across the vasculature and improves drug penetration in tumors. *Cancer Res*, **64**, 3731-6.

Willett CG, Boucher Y, Tomaso ED, et al (2004). Direct evidence that the VEGF-specific antibody bevacizumab has antivascular effects in human rectal cancer. *Nat Med*, **10**, 145-7.

Wildiers H, Guetens G, Boeck GD, et al (2003). Effect of antivascular endothelial growth factor treatment on the intratumoral uptake of CPT-11. *Br J Cancer*, **88**, 1979-86.